Műszaki Tudományos Közlemények vol. 20. (2024) 24–29.
DOI: Hungarian: https://doi.org/10.33895/mtk-2024.20.05
English: https://doi.org/10.33894/mtk-2024.20.05

GEAR HOB BASE WORM MODELLING FROM A STRAIGHT TOOTHED GENERATING RACK

Norbert HODGYAI,[1] Mircea VIOREL-DRĂGOI,[2] Márton MÁTÉ [3]

[1] *Transilvania University of Brașov, Faculty of Technological Engineering and Industrial Management, Department of Manufacturing Engineering, Romania, hodgyai@ms.sapientia.ro*

[2] *Transilvania University of Brașov, Faculty of Technological Engineering and Industrial Management, Department of Manufacturing Engineering, Romania, dragoi.m@unitbv.ro*

[3] *Sapientia Hungarian University of Transylvania, Faculty of Technical and Human Sciences, Mechanical Engineering Department, Tg. Mureș. Romania, mmate@ms.sapientia.ro*

Abstract

The precision of a gear realized by hobbing is mainly influenced by the precision of the base worm, the adequate form of the rake face and the number of resharpenings. Gearing theory states that the base worm of a gear hob must be of involute type. Despite of this, manufacturing technology often admits a convolute worm as gear hob base worm. Due to the rake face grinding technology, there appears a difference between the theoretical and the real surface. On the other hand, the profile modification of the cutting edges occurs due to the re-sharpening. As a result, the cutting edges cannot reproduce that initial basic worm surface from which the gear hob was derived. In our opinion, the computing of the generating surfaces of the basic worm is still an unsolved problem. This paper deals with the study of a worm derived from a straight toothed generating rack. The incidence of an involute worm and that developed from the generating rack is investigated.

Keywords*: gear hob, profile error, base worm, machining, generating rack.*

1. Introduction

Gear hobs are without any doubt nowadays the most productive gear cutting tools. They can be divided into three main groups: roughing, semi-finishing and finishing gear hobs. Finishing gear hobs are always realized in monolithic construction. A finishing gear hob's precision is imposed by the German standard **[1]**, grouping them in three classes denoted with AAA, AA and A, in decreasing order of their precision **[2, 3]**. A newer standard **[4]** was validate in 2020. Here, finishing gear hobs are grouped in four precision classes which in order of decreasing precision are 4A, 3A, 2A and finally, A.

The gear hob's precision is significantly influenced by the type and the machining precision level of the basic worm. When gear hob manufacturing is realized on classical machine tools, the involute basic worm is often replaced with a convolute one, because the manufacturing results are simpler and allow higher productivity **[5]**.

In order to reach the high precision class requirements and the optimization of durability, monolithic gear hobs are executed with helical rake faces **[6]**. Rake face grinding presents inevitable problems, resulting in the undercut phenomenon. The undercut here signifies that the grinding wheel sweeps away parts of the theoretical rake face, as proven by the mathematical model **[7, 8]**.

In this paper is analyzed the correspondence between a worm developed from a generating rack and a theoretical involute worm.

2. The mathematical model

2.1. Geometric basics

In this approach the thread surface of the generated worm is meshed by the tooth gap surfaces of the generating rack. The positions of the surfaces and the frames attached to them are represented in **Fig. 1.** Frame $O_2X_2Y_2Z_2$ is linked to the generating tooth gap of the rack.

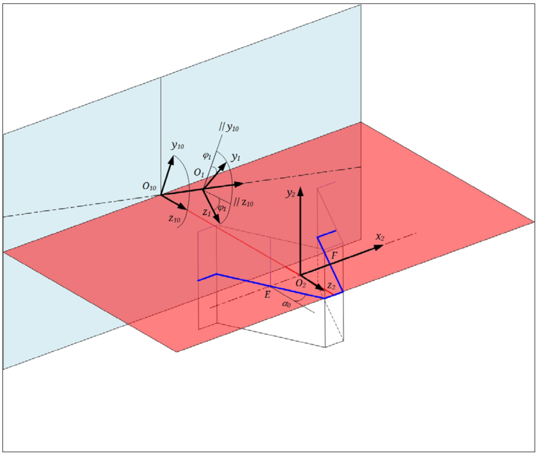

Fig. 1. *The geometrical model.*

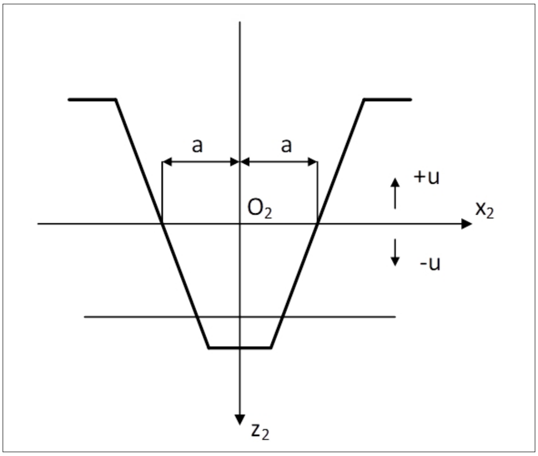

Fig. 2. *The key elements of the generating profile.*

The frame linked to the worm is $O_1X_1Y_1Z_1$ whose initial position is denoted by $O_1^0X_1^0Y_1^0Z_1^0$. Axis O_1x_1 of the worm closes the angle λ_0 with the motion direction of the rack.

This coincides with the declination angle of the worm's pitch helix. In this way, the tangent of the pitch helix coincides with the toothline direction of the rack. The relative motion of the worm compared to the rack is considered the helical motion of the worm about its own axis O_1x_1 characterized by helix parameter p.

Let us denote by φ_1 the rotation of the worm about its own axis. The generating lines of the tooth gap-surfaces are colored in blue. The profile angle of the rack is set on the standard value $\alpha_0 = 20°$.

In order to compute the equations of the worm surface the transformation matrix between the corresponding frames must be written. The matrix equation of the transformation is:

$$\underline{\mathbf{r}_1} = \mathbf{M}_{1 1^0} \cdot \mathbf{M}_{1^0 2} \cdot \underline{\mathbf{r}_2} \tag{1}$$

where

$$\mathbf{M}_{11^0} = \begin{pmatrix} 1 & 0 & 0 & -p\varphi_1 \\ 0 & \cos\varphi_1 & \sin\varphi_1 & 0 \\ 0 & -\sin\varphi_1 & \cos\varphi_1 & 0 \\ 0 & 0 & 0 & 1 \end{pmatrix} \tag{2}$$

$$\mathbf{M}_{1^0 2} = \begin{pmatrix} \cos\lambda_0 & -\sin\lambda_0 & 0 & 0 \\ \sin\lambda_0 & \cos\lambda_0 & 0 & 0 \\ 0 & 0 & 1 & r_{10} \\ 0 & 0 & 0 & 1 \end{pmatrix} \tag{3}$$

The parametric equations of the profile of the tooth gap are given by (**Fig. 2**):

$$\begin{cases} x_2(u; j) = j(a + u\,\mathrm{tg}\,\alpha_0) \\ y_2(v) = v \\ z_2(u) = -u \end{cases}, \quad a = \frac{\pi m}{4} \tag{4}$$

Parameter j is used as a unified representation for both flanks: $j = -1$ for the left side, and $j = +1$ for the right side. The left or right side is established observing the contrary of axis z_2 *as seen on* **Fig. 2.**

2.2. The solution of the equation of gearing

The equation of gearing is considered in Litvin's manner, in its vectorial form, and will be solved in the frame S_2 linked to the rack. Thus:

$$\mathbf{v}_2^{(12)} \cdot \mathbf{n}_2^{(2)} = 0 \tag{5}$$

The relative velocity vector is primed by the next equation

$$\mathbf{v}_2^{(12)} = \boldsymbol{\omega}_{O_2}^{(1)} \times (\mathbf{r}_2 - \mathbf{A}) + p\omega_1 \mathbf{i}_1 \tag{6}$$

The expressions of the specific terms are as follows. The angular velocity of the worm is:

$$\underline{\boldsymbol{\omega}_{O_2}^{(1)}} = \begin{pmatrix} \cos\lambda_0 \\ -\sin\lambda_0 \\ 0 \end{pmatrix} \tag{7}$$

The location vector of the worm's frame origin related to the frame of the rack is:

$$\underline{\mathbf{A}} = \begin{pmatrix} p\varphi_1 \cos\lambda_0 \\ -p\varphi_1 \sin\lambda_0 \\ -r_{10} \end{pmatrix} \quad (8),$$

After the substitution of vectors (7) and (8) in expression (7) and finishing the elementary calculus, the expression of the relative velocity results in the following form:

$$\mathbf{v}_2^{(12)} = \begin{pmatrix} -(r_{10}-u)\sin\lambda_0 + p\cos\lambda_0 \\ -(r_{10}-u)\cos\lambda_0 - p\sin\lambda_0 \\ j(a+u\,\mathrm{tg}\,\alpha_0)\sin\lambda_0 + v\cos\lambda_0 \end{pmatrix} \quad (9)$$

The normal vectors of the generating gap's surfaces are:

$$\mathbf{n}_2^{(2)} = \begin{pmatrix} j\cos\alpha_0 \\ 0 \\ \sin\alpha_0 \end{pmatrix} \quad (10)$$

Substituting vectors (9) and (10) in equation (5) results in a scalar equation of the form $\phi(u,v)=0$ which from parameter v can be expressed as follows:

$$v(u) = -j\,\mathrm{tg}\,\lambda_0 (a + \frac{u}{\sin\alpha_0 \cos\alpha_0}) \quad (11)$$

Using expression (11) in the matrix equation (1) the parametric equations of the worm thread surface are obtained in the following form:

$$\begin{cases} x_1(u,\varphi_1;j) = j\left(\dfrac{a}{\cos\alpha_0} + u\dfrac{\sin^2\alpha_0\cos^2\lambda_0 + \sin^2\lambda_0}{\sin\alpha_0\cos\alpha_0\cos\lambda_0}\right) \\ y_1(u,\varphi_1;j) = -j\,u\dfrac{\sin\lambda_0}{\mathrm{tg}\,\alpha_0}\cos\varphi_1 + (r_{10}-u)\sin\varphi_1 \\ z_1(u,\varphi_1;j) = j\,u\dfrac{\sin\lambda_0}{\mathrm{tg}\,\alpha_0}\sin\varphi_1 + (r_{10}-u)\cos\varphi_1 \end{cases} \quad (12)$$

Fig. 3. presents the worm thread surfaces realized in the MathCad environment. The following initial data were used: module $m = 5$ mm s and pitch helix angle $\lambda_0 = 2°$.

3. The investigation of the worm surfaces

3.1. Definition of the contact curve

The contact curve is the manifold of the common points of the generating surfaces and the meshed (the worm's) surfaces. Parametric equations of

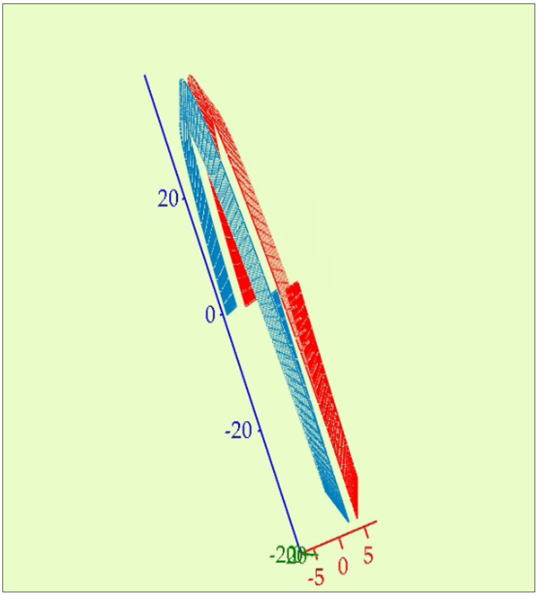

Fig. 3. *The worm thread surfaces*

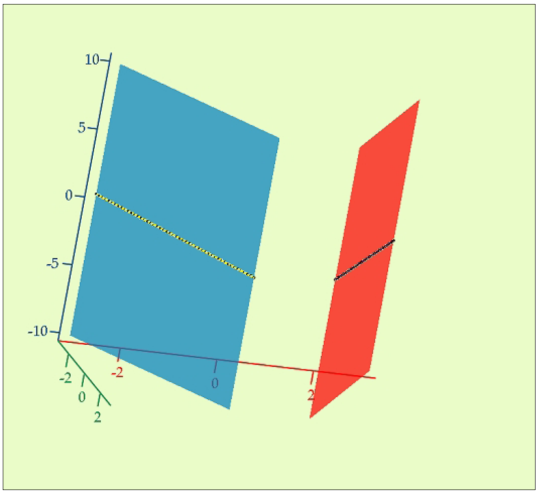

Fig. 4. *The generating surfaces and the contact lines*

the contact curve, related to the frame of the rack result by substituting parameter v in equations (4) (of the generating surfaces) by function *v(u)* expressed by equation (11). It results:

$$\begin{cases} x_2(u,j) = j\left(a + tg\alpha_0\right) \\ y_2(u,j) = -jtg\alpha_0\left(a + \dfrac{u}{\sin\alpha_0\cos\alpha_0}\right) \\ z_2(u,j) = -u \end{cases} \quad (13)$$

3.2. Computing of the frontal section of the worm

In order to simplify the calculus, it is useful and efficient to transpose the equations of the worm in cylindrical coordinates.

The following notations will be also introduced:

$$a_x = \frac{a}{\cos\lambda_0};\ b_x = \frac{\sin^2\alpha_0\cos^2\lambda_0 + \sin^2\lambda_0}{\sin\alpha_0\cos\alpha_0\cos\lambda_0}; \quad (14)$$

With these, equations (12) of the worm surfaces can be written in the following, simpler form:

$$\begin{cases} x_1(u,\varphi_1;j) = j\left(a_x + u b_x\right) - p\varphi_1 \\ y_1(u,\varphi_1;j) = -j\dfrac{\sin\lambda_0}{\operatorname{tg}\alpha_0}u\cos\varphi_1 + \left(r_{10} - u\right)\sin\varphi_1 \\ z_1(u,\varphi_1;j) = j\dfrac{\sin\lambda_0}{\operatorname{tg}\alpha_0}u\sin\varphi_1 + \left(r_{10} - u\right)\cos\varphi_1 \end{cases} \quad (15)$$

From these equations result the desired cylindrical coordinate form:

$$\begin{cases} \rho(u) = \left(y_1^2 + z_1^2\right)^{\frac{1}{2}} = \left(\dfrac{\sin^2\lambda_0}{\operatorname{tg}^2\alpha_0}u^2 + \left(r_{10} - u\right)^2\right)^{\frac{1}{2}} \\ \theta(u) = \operatorname{arctg}\dfrac{z_1}{y_1} = -\operatorname{tg}\left(\varphi_1 + \operatorname{arctg}\left(\dfrac{r_{10} - u}{u}\dfrac{\operatorname{tg}\alpha_0}{\sin\lambda_0}\right)\right) \\ x_1(u,\varphi_1;j) = j\left(a_x + u b_x\right) - p\varphi_1 \end{cases} \quad (16)$$

The frontal section of the worm can be obtained by intersecting its surfaces with a plane perpendicular to the axis. To simplify the result, let's consider plane $y_1O_1z_1$ for this purpose. Introducing an explicit equation of it in the third equation (16) results in a relation between parameters u and φ_1:

$$x_1 = 0 \ \Rightarrow\ \varphi_1 = j\frac{a_x + u b_x}{p} \quad (17)$$

By substituting φ_1 from (17) in equation (16) we obtain the polar equations of the worm's frontal profile:

$$\begin{cases} \rho(u) = \left(\dfrac{\sin^2\lambda_0}{\operatorname{tg}^2\alpha_0}u^2 + \left(r_{10} - u\right)^2\right)^{\frac{1}{2}} \\ \theta(u) = -\left(j\dfrac{a_x + u b_x}{p} + \operatorname{arctg}\left(\dfrac{r_{10} - u}{u}\dfrac{\operatorname{tg}\alpha_0}{\sin\lambda_0}\right)\right) \end{cases} \quad (18)$$

The careful investigation of parametric equations (18) leads to excluding the Archimedean worm type. First of all, function $\Theta(u)$ doesn't admit an explicit form of its inverse $u(\Theta)$ and even if such a function could exist, the resulting function couldn't be linear. On the other hand, the polar radius function $\rho(\Theta)$ is quadratic in u. Thus, linear dependence between $\rho(\Theta)$ and Θ could never be. Thus the hypothesis that the meshed helical surfaces are Archimedean helical surfaces is rejected.

3.3. Investigations regarding the relative positions of the contact lines and the worm's axis

A well-known peculiarity of an involute worm is that it is generated by two straight lines which lie in two parallel planes, both tangent to the basic cylinder whose radius is denoted by r_{1b}. The justifying calculus is driven in frame S_2 linked to the generating rack. The direction vectors of lines (13) are obtained by derivation by u:

$$\underline{\dot{r}_2} = \begin{pmatrix} j\operatorname{tg}\alpha_0 \\ -j\left(\dfrac{\operatorname{tg}\lambda_0}{\sin\alpha_0\cos\alpha_0}\right) \\ -1 \end{pmatrix} \quad (19)$$

The unit vector of the worm related to the frame S_2 (**Fig. 5.**) is:

$$\underline{\mathbf{i}_2^{(1)}} = \begin{pmatrix} \cos\lambda_0 \\ -\sin\lambda_0 \\ 0 \end{pmatrix} \quad (20)$$

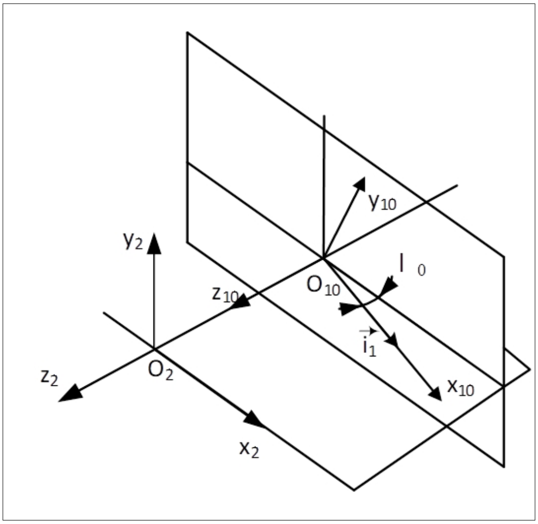

Fig. 5. *Ahe unit vector of the worm's axis.*

The common normal of $\dot{r}_2$ and $\mathbf{i}_2^{(1)}$ is obtained as a cross product of forms (19) and (20), written below in matrix form:

$$\underline{\mathbf{w}} = \left[\tilde{\mathbf{i}}_2^{(1)}\right]\underline{\dot{\mathbf{r}}_2} = \begin{pmatrix} \sin\lambda_0 \\ \cos\lambda_0 \\ -j\dfrac{\sin\lambda_0}{tg\alpha_0} \end{pmatrix} \tag{21}$$

Length of vector **w** results as:

$$|\mathbf{w}| = \sqrt{\sin^2\lambda_0 + \cos^2\lambda_0 + \frac{\sin^2\lambda_0}{\mathrm{tg}^2\alpha_0}} = \tag{22}$$

$$= \frac{\sqrt{\mathrm{tg}^2\alpha_0 + \sin^2\lambda_0}}{\mathrm{tg}\,\alpha_0}$$

From expressions (21) and (22) the components of the common normal unit vector result by a simple division:

$$\begin{aligned} w_{ex_2} &= \frac{\sin\lambda_0\,\mathrm{tg}\,\alpha_0}{\sqrt{\mathrm{tg}^2\alpha_0 + \sin^2\lambda_0}} \\ w_{ey_2} &= \frac{\cos\lambda_0\,\mathrm{tg}\,\alpha_0}{\sqrt{\mathrm{tg}^2\alpha_0 + \sin^2\lambda_0}} \\ w_{ez_2} &= -j\frac{\sin\lambda_0}{\sqrt{\mathrm{tg}^2\alpha_0 + \sin^2\lambda_0}} \end{aligned} \tag{23}$$

The axis with each of the contact lines form a pair of skew lines. For computing the distance between the skew lines it is necessary to pick a point in each one. On the axis of the worm the most appropriate is the origin whose coordinates in S_2 are:

$$O_1 = \begin{pmatrix} 0 & 0 & r_{10} \end{pmatrix} \tag{24}$$

where r_{10} is the pitch radius of the worm. Regarding the contact lines, the points resulting for $u=0$ were chosen. These points lie on axis O_2x_2:

$$\mathbf{A}_j = \underline{\mathbf{r}_2}(0) = \begin{pmatrix} ja \\ -ja\,\mathrm{tg}\,\lambda_0 \\ 0 \end{pmatrix} \tag{25}$$

In the following we define, using the points given by coordinates (24) and (25), the vector **P** which is as follows

$$\mathbf{P}_j = \overrightarrow{O_1A_j} = \begin{pmatrix} -ja \\ ja\,\mathrm{tg}\,\lambda_0 \\ r_{10} \end{pmatrix} \tag{26}$$

The distance between the skew lines, namely the axis and each one of the contact lines, is given by the scalar products of **P** vectors and the unit vector of **w**. With expressions (23) and (26) the distances result as follows:

$$d_j = \left|\mathbf{P}_j \cdot \frac{\mathbf{w}}{|\mathbf{w}|}\right| = \frac{r_{10}\sin\lambda_0}{\sqrt{\mathrm{tg}^2\alpha_0 + \sin^2\lambda_0}} \tag{27}$$

The literature of basic gear geometry presenting parts states that normal and frontal profile angles of a rack with inclined teeth are linked by the formula $\mathrm{tg}\,\alpha_{0t} = \mathrm{tg}\,\alpha_0/\cos\beta$, and by a transformation, it turns in:

$$\cos\alpha_{0t} = \frac{1}{\sqrt{1+\mathrm{tg}^2\alpha_{0t}}} = \frac{\cos\beta}{\sqrt{\cos^2\beta + \mathrm{tg}^2\alpha_{0t}}} \tag{28}$$

Admitting the equivalence between a worm and a gear with helical teeth, of a pitch helix angle of $\beta=\pi/2-\lambda_0$, and the number of teeth equal with the number threads of the worm, formula (28) turns in:

$$\cos\alpha_{0t} = \frac{\sin\lambda_0}{\sqrt{\cos^2\lambda_0 + \mathrm{tg}^2\alpha_{0t}}} \tag{29}$$

Looking simultaneously at formulae (27) and (29) it can be concluded that the distance between the contact lines and the axis of the worm are equal and meet the well- known value $r_{10}\cos\alpha_0$ which is the first basic formula of the involute trigonometry, as defined by Szeniczei.

Looking the calculus above it can be stated that the worm meshed by a straight toothed rack is an involute worm.

4. Conclusions

The investigation of the profile of the worm meshed by a straight toothed rack leads to an involute worm.

The contact between the meshed helical surfaces of the worm and the generating planes of the rack tooth gap is observed along straight segments.

References

[1] [DIN 3968] Tolerances for Single-start Hobs for Involute Spur Gears.

[2] Hollanda D.: *Aschiere si scule.* Reprografia I.I.S. Tg. Mures, 1982.

[3] Máté M.: *Hengeres fogaskerekek gyártószerszámai.* Erdélyi Múzeum-Egyesület, Kolozsvár, 2016.

[4] [ISO 4468 : 2020] Gear hobs – Accuracy Requirements.

[5] Radzevich, S. P.: *Gear Cutting Tools: Fundamentals of Design and Computation*. CRC Press; 1st edition, 2010.
[6] Radzevich, S. P.: *On the Accuracy of Precision Involute Hobs: An Analytical Approach*. Journal of Manufacturing Processes, 9/2. (2007) 121–136.
[7] Hodgyai N., Máté M., Tolvaly-R. F., Drăgoi M. V., *Peculiarities of the Grinding Process of a Gear Hob Helical Rake Face*. Acta Universitatis Sapientiae Electrical and Mechanical Engineering, 13. (2021) 39–51 https://doi.org/10.2478/auseme-2021-0004.
[8] Máté M., Tolvaly-R. F., Hodgyai N., Egyed-F. E.: *A csigamaró-homlokfelület köszörülésének valós modellje* („The Realistic Model of the Gear-Hob Rake face Grinding") 2022